RAA 2016 Vol. **16** No. **10**, 157 (8pp) doi: 10.1088/1674–4527/16/10/157
http://www.raa-journal.org *http://iopscience.iop.org/raa*

Research in Astronomy and Astrophysics

Photometric solution and period analysis of the contact binary system AH Cnc

Ying-Jiang Peng[1], Zhi-Quan Luo[1,†], Xiao-Bin Zhang[2], Li-Cai Deng[2], Kun Wang[2], Jian-Feng Tian[2], Zheng-Zhou Yan[2], Yang Pan[1], Wei-Jing Fang[1], Zhong-Wen Feng[4], De-Lin Tang[1], Qi-Li Liu[3], Jin-Jiang Sun[3] and Qiang Zhou[3]

[1] Physics and Space Science College, China West Normal University, Nanchong, 637002, China
[2] National Astronomical Observatories, Chinese Academy of Sciences, Beijing 100012, China; *nczqluo@126.com*
[3] Purple Mountain Observatory, Chinese Academy of Sciences, Nanjing 210008, China
[4] School of Physical Electronics, University of Electronic Science and Technology of China, Chengdu 610054, China

Received 2016 April 18; accepted 2016 June 27

Abstract Photometric observations of AH Cnc, a W UMa-type system in the open cluster M67, were carried out by using the 50BiN telescope. About 100 h of time-series B- and V-band data were taken, based on which eight new times of light minima were determined. By applying the Wilson-Devinney method, the light curves were modeled and a revised photometric solution of the binary system was derived. We confirmed that AH Cnc is a deep contact ($f = 51\%$), low mass-ratio ($q = 0.156$) system. Adopting the distance modulus derived from study of the host cluster, we have re-calculated the physical parameters of the binary system, namely the masses and radii. The masses and radii of the two components were estimated to be respectively $1.188(\pm0.061)\,M_\odot$, $1.332(\pm0.063)\,R_\odot$ for the primary component and $0.185(\pm0.032)\,M_\odot$, $0.592(\pm0.051)\,R_\odot$ for the secondary. By adding the newly derived minimum timings to all the available data, the period variations of AH Cnc were studied. This shows that the orbital period of the binary is continuously increasing at a rate of $dp/dt = 4.29 \times 10^{-10}$ d yr^{-1}. In addition to the long-term period increase, a cyclic variation with a period of 35.26 yr was determined, which could be attributed to an unresolved tertiary component of the system.

Key words: methods: data analysis — astronomical instrumentation — binaries: eclipsing stars, close stars — Galaxy: open clusters and associations: individual (M67)

1 INTRODUCTION

Galactic open clusters (hereafter OCs) are ideal laboratories for stellar astrophysics because they offer a unique opportunity to observe structures, interactions and dynamical evolutions of stellar systems, and even of the Galaxy. They can also test the theory of stellar evolution in a delicate way, as modern observational technology progresses. The benchmark cluster M67, in particular, is an old OC with an age of about 4 Gyr (Fan et al. 1996; Davenport & Sandquist 2010). This cluster is important for its richness of member stars, old age and the fact that it is populated with all types of special objects. There are over 1000 member stars in this OC (Qian et al. 2006a), including at least seven W UMa stars (Sandquist & Shetrone 2003b); a significant number are blue stragglers (hereafter BS), with about 60 percent of BS in binaries; in addition, a good proportion radiate in X-ray; and there are a red straggler and two subgiants. These variables undoubtedly provide us with lots of very valuable information to study the structures and evolutions of these stars and their host cluster.

Deep, low mass ratio overcontact binary stars are a special sub-group of W UMa binaries, whose degrees of overcontact are normally larger than 50% and mass ratios are less than 0.25. More research work can be found in (Qian et al. 2005a, 2006b).

AH Cnc, a member star in M67, is a relatively bright eclipsing binary with a large amplitude of light variation. It is also the first known and a heavily studied variable star in this OC. Its variability was discovered by Kurochkin (1960), and was later identified as a W UMa system by Efremov et al. (1964). Interestingly, this binary was once misclassified as an RR Lyrae variable star by Kurochkin (1960), which was later noted by Maceroni et al. (1984) who reported that this system is actually a W-type overcontact binary system instead. However, recent works, such as Sandquist & Shetrone (2003a), Zhang et al. (2005) and Qian et al. (2006a), have shown that this binary is an A-type system. The spectral type of AH Cnc was assigned to be F7V (Maceroni et al. 1984).

† Corresponding author.

2 CCD PHOTOMETRIC OBSERVATIONS

CCD photometric observations of AH Cnc were made with the 50BiN prototype telescope which has two parallel camera systems with two standard Johnson-Cousins-Bessell BV filters. Both cameras are Andor DZ936, with a 2k×2k CCD detector, and they offer a $20' \times 20'$ clear field of view. Simultaneous two-color photometric observations are possible with the binocular design. The exposure times were set as 60 s for V-band and 150 s for B-band. Observations were carried out over 23 nights (from 2014 Feb. 19 to 2015 Mar. 20), which gave a total exposure time of about 100 h. High quality time series photometric data were produced from that observation run. We obtained a total of 7546 frames including 5052 V-band and 2494 B-band images. The observation log is provided in Table 1, and some time series representing light curves are shown in Figure 1.

An automated photometry data reduction pipeline, mainly based on the DAOPHOT II software package (Stetson 1987), was employed to subtract bias frames, correct flat fields, calibrate astrometry and extract photometry. The same procedure has been thoroughly tested using 50BiN in the study of NGC 2301 (Wang et al. 2015). To obtain the B and V standard magnitudes, 30 unsaturated and isolated bright stars which must show long-term stability during the observations were selected as the secondary standards. A cross-identification (Eq. (1) and Eq. (2)) between these secondary standards and the data reported by Yakut et al. (2009) was employed. Calibrating against the 30 secondary standards and allowing a linear transformation, using these instrumental magnitudes which are from several images taken under photometric conditions, the standard magnitudes and colors of stars in the whole field were then obtained.

$$B_0 = B + a \times (B - V) + b, \tag{1}$$

$$V_0 = V + c \times (B - V) + d, \tag{2}$$

where B_0 and V_0 are the standard magnitudes from Yakut et al. (2009), while B and V are the instrumental magnitudes. The coefficients a, b, c and d are parameters to be determined by the fitting process.

A normalization technique was employed to calibrate the instrumental magnitudes of time-series frames as described by Gilliland & Brown (1988). We extracted the light curves of individual stars in the field of M67 in the following way: For the V and B filters, the same 30 standard stars were used for the calibration. We used the following equation (Eq. (3)) to transform the instrumental data v of each time-series V-band frame to the standard magnitude in V

$$V = v + a_1 + a_2(B - V) + a_3X + a_4Y, \tag{3}$$

where X and Y are a star's positions on a CCD frame. The coefficients a_1, a_2, a_3 and a_4 computed by the least-squares method are different for different frames. The mid-exposure time of each measurement was converted to HJD. All of the detected stars on each image were calibrated using the above equation.

3 LIGHT CURVES AND PERIOD CHANGES

To assess the period variation of AH Cnc, eight new minimum times were determined and they are listed in Table 2. A new linear ephemeris was obtained which is shown in Equation (4). For this system, the period was determined to be 0.360452 d from van den Berg et al. (2002), 0.36045754 d from Zhang et al. (2005) and 0.3604583 d from Yakut et al. (2009). We derived a new period of 0.3604607 d, based on the phased light curves of all the new measurements. In the current work, the primary minimum of phased curves was defined as the moment when the massive component is osculated by the less massive component, like in other studies. The following equation is the new linear ephemeris based on those minimum times,

$$\text{Min.I} = \text{HJD}2457044.1667^{\text{d}} + 0.3604607^{\text{d}} \times E. \tag{4}$$

Figure 2 is V-band time series light curve of every night. The phased B- and V-band light curves with a starspot are shown in Figure 3. The phased time series in the form of a light curve for all nights with data that were used in V-band is displayed in Figure 2. Based on a probable quadratic variation of period change shown in the $O - C$ plot, a quadratic ephemeris can be given as the following (Eq. (5)),

$$\begin{aligned} \text{Min.I} \;=\; & \text{HJD}2457044.1858^{\text{d}} + 0.360477^{\text{d}} \times E \\ & + 2.9173 \times 10^{-10} E^2. \end{aligned} \tag{5}$$

It is clearly shown by the phased light curves (Fig. 3) that the bottoms of the secondary eclipses in both B- and V-bands are rather flat, and cover approximately 0.1 of an orbital phase. A flat bottom in primary eclipse was also found in the B-band light curve. However, there seemed to be no flat feature in the V-band curve. As demonstrated by Qian et al. (2006a), a typical O'Connell effect was obviously shown in their light curves, but the same phenomenon was not confirmed by the current observational data. The primary maximum is only 0.0027 mag higher than the secondary one in V-band and 0.0024 mag higher in B-band. There is also no increase in brightness before maximum as in Sandquist & Shetrone (2003a).

For assessing the period variation of AH Cnc, the epoch and $O - C$ residuals were calculated and the results are listed in Table 4. Qian et al. (2006a) and Kreiner et al. (2001) found that there is a complex variation and a continuous period change in this system; such a phenomenon is also detected in our work. An equation of $(O-C)_1$ variation with no sinusoidal term was applied at the beginning. A poor fitting result, shown in Figure 4, was obtained. A regular shift was therefore implied in the residuals (the bottom of Fig. 4). Then, a sinusoidal variation was added to get a better description of the $(O - C)_1$ data (Fig. 4, red line). By assigning a weight of 10 to the V, R, I photometric and CCD data (Table 4, the 'Method'), a least-squares

Table 1 Journal of the Observations

Date	HJD (+2450000)	Obs.time (h)	Frames (V)	Frames (B)	Exp.time (s)
2014 Feb. 19	6708.061	6.67	463	259	40
2014 Dec. 06	6998.333	3.00	157	65	90
2014 Dec. 14	7006.408	1.20	69	29	60
2014 Dec. 15	7007.422	1.15	68	29	60
2014 Dec. 16	7008.205	6.67	201	139	60
2014 Dec. 17	7009.218	6.28	351	147	60
2015 Jan. 20	7043.097	7.89	453	189	60
2015 Jan. 21	7044.106	7.63	428	180	60
2015 Jan. 22	7045.104	7.82	353	140	60
2015 Jan. 23	7046.236	4.54	292	122	60
2015 Jan. 24	7047.165	6.22	348	146	60
2015 Feb. 07	7061.219	3.89	223	93	60
2015 Feb. 08	7062.281	2.33	137	57	60
2015 Feb. 10	7064.166	5.04	284	119	60
2015 Feb. 11	7065.268	2.50	143	59	60
2015 Mar. 01	7083.078	3.96	386	162	60
2015 Mar. 10	7092.162	3.12	176	73	60
2015 Mar. 11	7093.051	4.73	274	115	60
2015 Mar. 12	7094.055	4.82	307	129	60
2015 Mar. 13	7095.034	0.77	46	19	60
2015 Mar. 20	7102.036	5.13	290	122	60

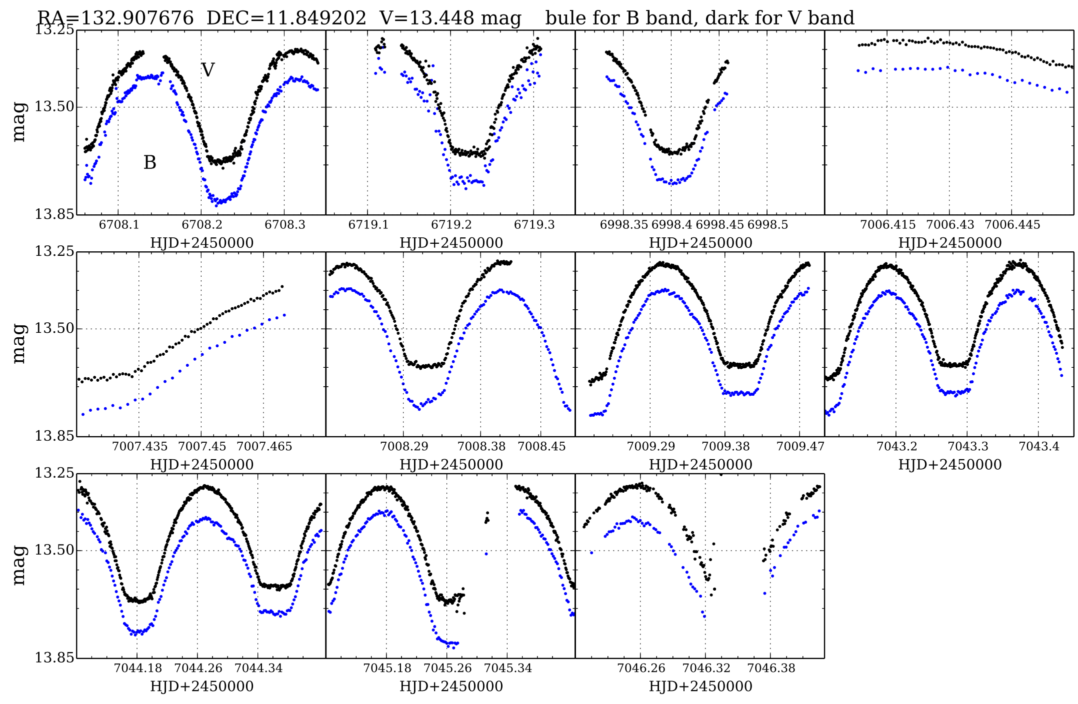

Fig. 1 The time series representing the light curve in the V- and B-bands.

solution yields the following equation (Eq. (6))

$$\begin{aligned}(O-C)_1 \;=\; & 0.0277 - 9.28\times10^{-6}E \\ & +2.12\times10^{-10}E^2 \\ & +0.0610\sin(0.000176E+2.49). \qquad (6)\end{aligned}$$

A long-term period increase at the rate of $dp/dt = 4.29\times10^{-9}$ d yr^{-1} was indicated in the quadratic term in Equation (6), which means that the period of AH Cnc increased at a rate of about 3.71 s per century. The sinusoidal term corresponds to a cyclic oscillation with an amplitude of 0.0610 d and a period of 35.26 yr.

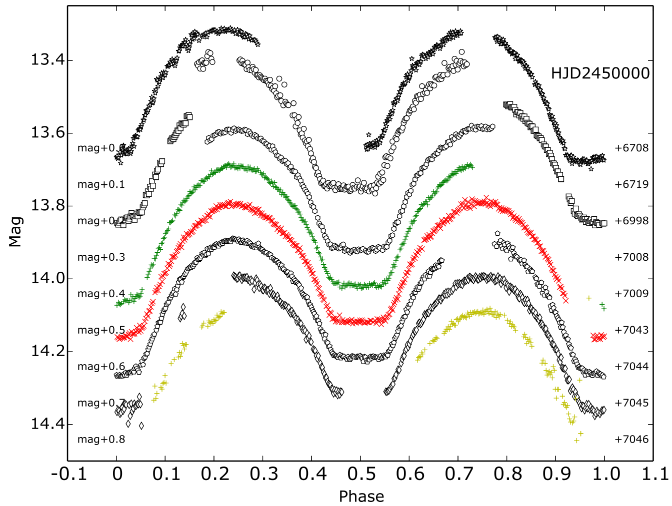

Fig. 2 The phased light curves of AH Cnc in the V-band for all nights with observing time longer than 4.5 h (more than half of the orbital period). No obvious O'Connell effect was detected in the data.

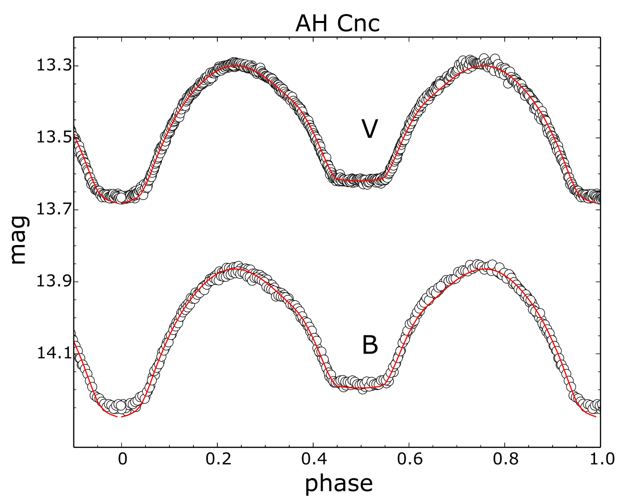

Fig. 3 The phased V-band light curve with a spot on the primary component. In fact, there is neither an obvious O'Connell effect in both V- and B-bands as previously reported by Qian et al. in 2006, nor is there any detectable brightness increase before maximum, as published by Sandquist and Shetrone in 2003.

Table 2 New Times of Minimum

Minimum (+2450000)	Uncertainty
6708.211472	±1.81 E–04
6719.222626	±1.71 E–04
6998.398468	±3.10 E–04
7008.310059	±1.37 E–04
7009.397766	±7.65 E–05
7043.281189	±8.90 E–05
7044.181335	±2.98 E–04
7044.363159	±1.55 E–04

In Figure 4, the red line represents the fitting by Equation (6) in the upper window. The residuals are listed in the sixth column of Table 4 and are shown in Figure 4 (the bottom panel). As displayed in the bottom panel of Figure 4 and Table 4, the scatters of those residuals associated with the observations are rather large (up to 0.00586 d). We would like to argue that the large scatter cannot be simply attributed to variations in the light curves due to starspot activity on the components (e.g., Kalimeris et al. 2002; Qian et al. 2006a) or the effect of asymmetry in the orbit of the system. A third component is very likely to exist in this system.

4 PHOTOMETRIC SOLUTION

In order to derive reliable photometric parameters, the 2003 version of the Wilson-Devinney code was employed. Light curves were transformed into normal points with an

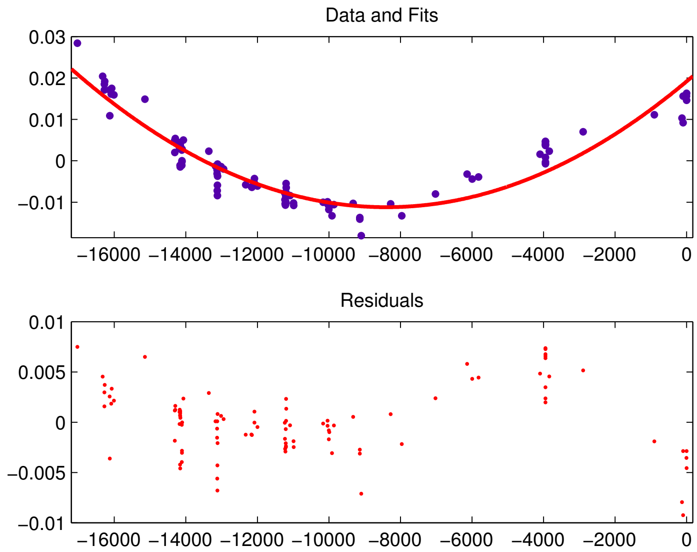

Fig. 4 A preliminary fitting (*upper panel*), leaving a scatter with an obvious $\sin$ pattern (*lower panel*) that cannot be attributed to a starspot or asymmetry in the system. A pattern of variation is shown in the bottom, which features some periodicity that could be fitted by adding a sinusoidal signal (also see Fig. 5).

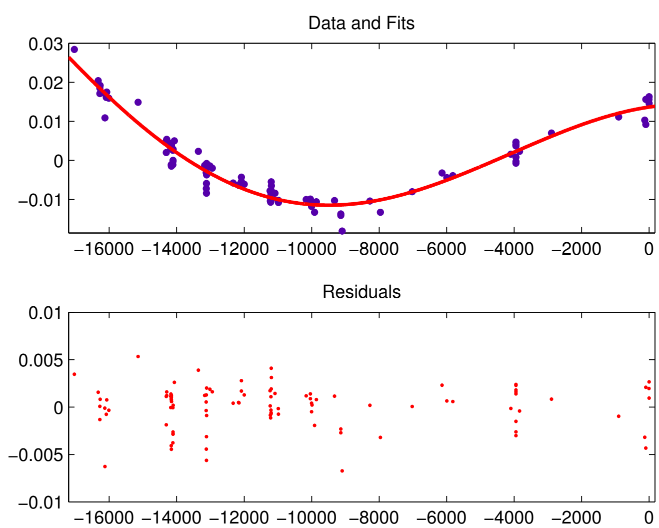

Fig. 5 The purple points in the upper panel are from residuals of $(O-C)_1$ (Fig. 4), and the red line corresponds to the periodic term in Eq. (3). The red points on the lower panel are the residuals. There is no longer an obvious pattern in this residual plot (*lower panel*).

average interval of 0.005 in phase. About 200 points were obtained. These points were then inserted in dcin.active.

AH Cnc is an A-type binary system (Zhang et al. 2005; Qian et al. 2006a), and the spectral type is F7V (Whelan et al. 1979). According to Cox & Pilachowski (2000), the temperature of the primary component is accepted to be $T_1 = 6300$ K. From Lucy (1967), the gravity-darkening exponents are set as $g_1 = g_2 = 0.32$.

Following Rucinski (1969), albedos of this system were adopted as $A_1 = A_2 = 0.5$. Based on the result of Diaz-Cordoves et al. (1995), the limb-darkening coefficient is chosen as 0.640. Mode 3 is employed in the DC program of the Wilson-Devinney (hereafter W-D) code in this work. The adjustable parameters include the orbital inclination i, the temperature of the secondary star T_2, the potentials Ω_1 and Ω_2 of two member components, and the non-dimensional luminosities L_1 and L_2. Some of the main parameters of V- and B-band light curves are given in Table 3.

The most sensitive parameter of light curve synthesis, mass ratio $q = M_1/M_2$, for AH Cnc, still remains uncertain. Earlier than the current work, Whelan et al. (1979)

Table 3 Photometric Solutions for AH Cnc

Parameter	Value	Uncertainty
$T1$ (K)	6300	assumed
$T2$ (K)	6151	±25
$\Omega_{\rm in}$	2.1300	...
$\Omega_{\rm out}$	2.0269	...
$\Omega_1 = \Omega_2$	2.075	±0.0017
i (°)	83.108	±0.002
$L1/(L1+L2)$	0.886	±0.071
$q = m2/m1$	0.156	assumed
$r1$ (pole)	0.5164	±0.0004
$r1$ (side)	0.5710	±0.0007
$r1$ (back)	0.5953	±0.0008
$r2$ (pole)	0.2299	±0.0005
$r2$ (side)	0.2409	±0.0006
$r2$ (back)	0.2887	±0.0015
Latitude spot (deg)	00.9785	±0.8196
Longitude spot (deg)	02.0889	±0.3197
Radius spot (deg)	00.0486	±0.0321
Tspot$/T$	00.8967	0.3253

and Maceroni et al. (1984) conducted a study trying to work out this value and their result only yielded a range from 0.4 to 0.7. Later, Sandquist & Shetrone (2003a) gave a smaller value of 0.157. Then, Zhang et al. (2005) published a result of 0.149, and Qian et al. (2006a) quoted a value of 0.1682. The latest published mass ratio is 0.168 (Yakut et al. 2009). As is well known, matching a light curve with a total eclipse requires a low mass ratio, therefore the results of Sandquist & Shetrone (2003a), Zhang et al. (2005), Qian et al. (2006a) and Yakut et al. (2009) would likely be more reliable.

In this work, mass ratios ranging from 0.1 to 0.7 were tested to find the most appropriate number. We let the mass ratio be freely adjustable along with the other free parameters and ran the W-D code again. In that way we got the best-fitting solution, which turned out to be 0.156.

Assuming there is a spot on the primary component (the massive one), we synthesized the asymmetry of the light curve. The mean parameters of this spot are co-latitude and longitude, radius R_s and temperature T_s, which were calculated by adjusting the theoretical light curves to approximately fit the observed distorted light curves. The final photometric solutions for both the B- and V-band light curves were obtained in this way. The result is given in Table 3, and the light curve from the final solution is plotted as a red line in Figure 3.

In order to derive reliable masses for both components, a method depending on the distance modulus was used because there are no radial velocity measurements for this system available from the literature. Fortunately, the distance modulus of M67 is well studied, which can be applied directly to AH Cnc. Starting with the known distance modulus of M67, $(m-M)_V = 9.72 \pm 0.05$ from Sandquist (2004), the maximum magnitude of the V-band is $V_{\rm max} = 13.292$, and $BC = 0.008$, corresponding to the spectral type of F7V (Whelan et al. 1979). When combined with the photometric solution from Table 3, as well as the known orbital period, the masses and radius of AH Cnc were then estimated as $1.18(\pm0.08)\,M_\odot$, $1.332(\pm0.06)\,R_\odot$ for the primary component and $0.185(\pm0.03)\,M_\odot$, $0.592(\pm0.051)\,R_\odot$ for the second one.

5 RESULTS AND DISCUSSION

CCD photometric data of the W UMa-type binary system AH Cnc, in the open cluster M67, were obtained from February 2014 to March 2015. The B- and V-band time-series light curves (Fig. 1) including eight new times of minima (Table 2) have been determined. Based on these time series in the form of light curves, a complete phased light curve is also shown in Figure 3. The photometric parameters of AH Cnc have been calculated and are listed in Table 3. The solutions of the system indicate that AH Cnc is a deep overcontact binary system ($f = 51\%$) that undergoes total eclipses with a small mass ratio of $q = 0.156$.

The photometric solutions show that AH Cnc, just like FG Hya (Qian & Yang 2005), EM Psc (Qian et al. 2008) and V1191 Cyg (Zhu et al. 2011), has changed into an A-type binary from a W-type, where the more massive component is hotter than the less massive one.

The masses and radii of both components are calculated to be $1.188(\pm0.06)\,M_\odot$, $1.332(\pm0.06)\,R_\odot$ for the primary component and $0.185(\pm0.03)\,M_\odot$, $0.592(\pm0.051)\,R_\odot$ for the secondary, respectively. The results agree well with other results in Qian et al. (2006a) and Zhang et al. (2005).

A cyclic sinusoidal variation with period of 35.26 years and amplitude of 0.0610 d are evident in the orbital period of AH Cnc by combining eight new determinations of minima and all of the available detections from literature. This term of the new $(O-C)$ equation demonstrates

Table 4 Photometric Solutions for AH Cnc

HJD +2450000	E	Method	$(O-C)_1$	Residuals	Reference	HJD +2450000	E	Method	$(O-C)_1$	Residuals	Reference
50904.2880	−17033.5	ccd	0.0028	0.0234	Roger	51159.3059	−16326.0	ccd	−0.0027	0.0141	Youn
51177.1469	−16276.5	ccd	−0.0043	0.0092	Youn	51177.3257	−16276.0	ccd	−0.0058	0.0048	Youn
51179.3103	−16270.5	ccd	−0.0037	0.0115	Youn	51229.7727	−16130.5	ccd	−0.0053	0.0079	Blake
51231.7490	−16125.0	ccd	−0.0115	−0.012	Blake	51245.8122	−16086.0	ccd	−0.0061	0.0056	Blake
51250.6798	−16072.5	ccd	−0.0047	0.0103	Blake	51273.0268	−16010.5	ccd	−0.0060	0.0066	Youn
51585.1847	−15144.5	V	−0.0040	0.0204	Szilar	51886.8804	−14307.5	V	−0.0109	0.0035	Sandquist
51887.0577	−14307.0	V	−0.0138	−0.0060	Sandquist	51890.8459	−14296.5	V	−0.0104	0.0050	Sandquist
51891.9269	−14293.5	V	−0.0108	0.0037	Sandquist	51933.7395	−14177.5	V	−0.0112	0.0031	Sandquist
51933.9186	−14177.0	V	−0.0124	−0.0007	Sandquist	51935.9025	−14171.5	V	−0.0110	0.00379	Sandquist
51939.1411	−14162.5	ccd	−0.0165	−0.0135	Qian	51939.8670	−14160.5	V	−0.0115	0.0021	Sandquist
51940.2221	−14159.5	ccd	−0.0169	−0.0147	Qian	51940.2278	−14159.5	ccd	−0.0112	0.0033	Qian
51940.7683	−14158.0	V	−0.0113	0.0027	Sandquist	51940.9482	−14157.5	V	−0.0117	0.0018	Sandquist
51941.8492	−14155.0	V	−0.0118	0.0012	Sandquist	51956.9876	−14113.0	ccd	−0.0126	−0.0010	Zhang
51957.1642	−14112.5	ccd	−0.0162	−0.0127	Zhang	51958.0662	−14110.0	ccd	−0.0154	−0.0098	Zhang
51958.2465	−14109.5	ccd	−0.0153	−0.0098	Zhang	51959.1478	−14107.0	ccd	−0.0152	−0.0091	Zhang
51959.8715	−14105.0	V	−0.0124	−0.0002	Sandquist	51972.6701	−14069.5	V	−0.0100	0.0073	Sandquist
52228.9549	−13358.5	V	−0.0102	0.0090	Sandquist	52296.7179	−13170.5	V	−0.0132	0.0002	Sandquist
52311.6762	−13129.0	V	−0.0138	−0.0021	Sandquist	52311.8555	−13128.5	V	−0.0148	−0.0050	Sandquist
52314.1944	−13122.0	ccd	−0.0188	−0.0179	Qian	52314.2001	−13122.0	ccd	−0.0131	0.0002	Zhang
52315.0943	−13119.5	ccd	−0.0201	−0.0216	Qian	52315.2771	−13119.0	ccd	−0.0175	−0.0137	Qian
52316.7240	−13115.0	V	−0.0124	0.0025	Sandquist	52316.9013	−13114.5	V	−0.0154	−0.0067	Sandquist
52352.7695	−13015.0	V	−0.0126	0.0018	Sandquist	52378.7220	−12943.0	V	−0.0131	0.0008	Sandquist
52600.9423	−12326.5	V	−0.0146	−0.0041	Sandquist	52657.8945	−12168.5	I	−0.0146	−0.0040	Sandquist
52662.9409	−12154.5	I	−0.0146	−0.0041	Sandquist	52688.7148	−12083.0	I	−0.0134	−0.0003	Sandquist
52688.8962	−12082.5	I	−0.0122	0.0032	Sandquist	52719.7138	−11997.0	I	−0.0137	−0.0016	Sandquist
52995.2842	−11232.5	ccd	−0.0128	−0.0003	Zhang	52996.3640	−11229.5	ccd	−0.0143	−0.0053	Zhang
52997.2642	−11227.0	ccd	−0.0153	−0.0085	Zhang	53001.2290	−11216.0	ccd	−0.0155	−0.0093	Zhang
53004.2951	−11207.5	ccd	−0.0133	−0.0023	Zhang	53005.1948	−11205.0	ccd	−0.0147	−0.0067	Zhang
53005.3747	−11204.5	ccd	−0.0151	−0.0077	Zhang	53006.2758	−11202.0	ccd	−0.0151	−0.0079	Zhang
53007.1818	−11199.5	ccd	−0.0102	0.0072	Zhang	53008.2609	−11196.5	ccd	−0.0125	0.0003	Zhang
53009.3435	−11193.5	ccd	−0.0113	0.0041	Zhang	53047.3702	−11088.0	ccd	−0.0128	−0.0011	Krajci T
53083.0540	−10989.0	ccd	−0.0143	−0.0061	Qian	53084.1348	−10986.0	ccd	−0.0148	−0.0079	Qian
53380.2541	−10164.5	V	−0.0111	−0.0005	Kazuhi	53426.3926	−10036.5	ccd	−0.0111	−0.0012	Qian
53426.3931	−10036.5	ccd	−0.0106	0.0004	Krajci	53426.3931	−10036.5	R	−0.0106	0.0004	Yakut K
53437.7466	−10005.0	ccd	−0.0115	−0.0026	Tom	53439.1876	−10001.0	ccd	−0.0123	−0.0055	Qian
53442.7929	−9991.0	ccd	−0.0116	−0.0032	Robert	53471.0869	−9912.5	ccd	−0.0135	−0.0098	Qian
53489.2928	−9862.0	R	−0.0106	−0.0011	Yakut K	53683.5814	−9323.0	R	−0.0084	0.0016	Yakut K
53750.6233	−9137.0	I	−0.0116	−0.0100	Yakut K	53750.6237	−9137.0	V	−0.0112	−0.0087	Yakut K
53750.6237	−9137.0	R	−0.0112	−0.0087	Yakut K	53765.3982	−9096.0	VI	−0.0154	−0.0225	Szliar
54060.9837	−8276.0	R	−0.0047	0.0025	Robert	54173.4445	−7964.0	ccd	−0.0066	−0.0069	Schmidt U
54513.3642	−7021.0	$-Ir$	0.0021	0.0075	Manfred	54831.8360	−6137.5	V	0.0100	0.0183	Roger
54883.7412	−5993.5	ccd	0.0094	0.0136	Robert	54946.6421	−5819.0	V	0.0105	0.0140	Shawn
55567.0004	−4098.0	V	0.0221	0.0153	Roger	55621.4321	−3947.0	R	0.0248	0.0201	Agerer Franz
55621.4323	−3947.0	B	0.0250	0.0208	Agerer Franz	55621.4325	−3947.0	I	0.0252	0.0214	Agerer Franz
55621.4330	−3947.0	V	0.0257	0.0230	Agerer Franz	55621.4331	−3947.0	$-Ir$	0.0258	0.0233	Agerer Franz
55625.4152	−3936.0	ccd	0.0428	*assumed*	Schmidt U	55649.3804	−3869.5	ccd	0.0376	*assumed*	Schmidt U
55660.7209	−3838.0	V	0.0237	0.0144	Roger	56001.7214	−2892.0	V	0.0318	0.0163	Roger
55621.4277	−3947.0	V	0.0204	0.0062	B.R.N.O.	55621.4281	−3947.0	R	0.0208	0.0075	Trnka J
55621.4292	−3947.0	I	0.0219	0.0110	Trnka J	56708.2267	−932.0	ccd	0.0411	−0.0060	
56719.2225	−901.5	ccd	0.0430	−0.0252		56998.4104	−127.0	ccd	0.0569	−0.0293	
57008.3124	−99.5	ccd	0.0463	*assumed*		57009.3978	−96.5	ccd	0.0503	−0.0091	
57043.2975	−2.5	ccd	0.0670	−0.0112		57044.1823	−0.0	ccd	0.0507	−0.0145	
57044.3633	0.5	ccd	0.0515	−0.0091							

Notes: *assumed* means that this point was deleted because of its large scatter when we calculated the period change. Some data are from *http://var2.astro.cz/ocgate/*.

that there could be a third component in this system. If this conclusion is true, then a large amount of angular momentum would be taken away from the binary system by this third component, and this central binary would have a short initial orbital period.

The general trend of the $O-C$ curve in Figure 5 indicates that the system undergoes a long-term increase in period at a rate of $dp/dt = 4.29 \times 10^{-9}$ d yr^{-1}. In other words, the period of AH Cnc increases by 3.71 s in a century. A plausible scenario would be that mass transfer from the less massive component to the more massive one has been happening. We can insert the absolute masses of both components into the well known equation (Eq. (7))

$$\dot{P}/P = 3\dot{M}_2(1/M_2 - 1/M_1)\,. \tag{7}$$

The mass transfer ratio is $dM_2/dt = 8.7 \times 10^{-10}\ M_\odot\ \mathrm{yr}^{-1}$. This may be used to infer that, just like V410 Aurigae (Yang et al. 2005), V835 Herculis (Qian et al. 2005b), QX Andromedae (Qian et al. 2007) and EM Piscium (Qian et al. 2008), AH Cnc will eventually evolve and merge into a rapidly rotating single star.

Acknowledgements This work is supported by the National Natural Science Foundation of China (Nos. U1131121, 11303021, U1231202, 11473037 and 11373073).

References

Ahumada, J., & Lapasset, E. 1995, A&AS, 109
Cox, A. N., & Pilachowski, C. A. 2000, Physics Today, 53, 77
Davenport, J. R. A., & Sandquist, E. L. 2010, ApJ, 711, 559
Deng, L., Chen, R., Liu, X. S., & Chen, J. S. 1999, ApJ, 524, 824
Diaz-Cordoves, J., Claret, A., & Gimenez, A. 1995, A&AS, 110, 329
Efremov, Y. N., Kholopov, P. N., Kukarkin, B. V., & Sharov, A. S. 1964, Information Bulletin on Variable Stars, 75, 1
Fan, X., Burstein, D., Chen, J.-S., et al. 1996, AJ, 112, 628
Gilliland, R. L., & Brown, T. M. 1988, PASP, 100, 754
Hurley, J. R. 2007, Highlights of Astronomy, 14, 442
Kalimeris, A., Rovithis-Livaniou, H., & Rovithis, P. 2002, A&A, 387, 969
Kreiner, J. M., Kim, C.-H., & Nha, I.-S. 2001, An Atlas of O–C Diagrams of Eclipsing Binary Stars (Cracow, Poland: Wydawnictwo Naukowe Akademii Pedagogicznej)
Kurochkin, N. E. 1960, Astronomicheskij Tsirkulyar, 212, 9
Lucy, L. B. 1967, ZAp, 65, 89
Maceroni, C., Milano, L., & Russo, G. 1984, A&AS, 58, 405
Mathieu, R. D., van den Berg, M., Torres, G., et al. 2003, AJ, 125, 246
Milone, A. A. E., & Latham, D. W. 1992, in IAU Symposium, Vol. 151, Evolutionary Processes in Interacting Binary Stars, ed. Y. Kondo, R. Sistero, & R. S. Polidan, 475
Qian, S.-B., He, J.-J., Soonthornthum, B., et al. 2008, AJ, 136, 1940
Qian, S.-B., Liu, L., Soonthornthum, B., Zhu, L.-Y., & He, J.-J. 2006a, AJ, 131, 3028
Qian, S.-B., Liu, L., Soonthornthum, B., Zhu, L.-Y., & He, J.-J. 2007, AJ, 134, 1475
Qian, S.-B., Yang, Y.-G., Soonthornthum, B., et al. 2005a, AJ, 130, 224
Qian, S.-B., Zhu, L.-Y., Soonthornthum, B., et al. 2005b, AJ, 130, 1206
Qian, S., & Yang, Y. 2005, MNRAS, 356, 765
Qian, S., Yang, Y., Zhu, L., He, J., & Yuan, J. 2006b, Ap&SS, 304, 25
Rucinski, S. M. 1969, Commmunications of the Konkoly Observatory Hungary, 65, 361
Sandquist, E. L. 2004, MNRAS, 347, 101
Sandquist, E. L., & Shetrone, M. D. 2003a, AJ, 126, 2954
Sandquist, E. L., & Shetrone, M. D. 2003b, AJ, 125, 2173
Stetson, P. B. 1987, PASP, 99, 191
van den Berg, M., Stassun, K. G., Verbunt, F., & Mathieu, R. D. 2002, A&A, 382, 888
Wang, K., Deng, L., Zhang, X., et al. 2015, AJ, 150, 161
Whelan, J. A. J., Romanishin, W., Worden, S. P., & Rucinski, S. M. 1979, MNRAS, 186, 729
Yakut, K., Zima, W., Kalomeni, B., et al. 2009, A&A, 503, 165
Yang, Y. G., Qian, S. B., Gonzalez-Rojas, D. J., & Yuan, J. Z. 2005, Ap&SS, 300, 337
Zhang, X. B., Zhang, R. X., & Deng, L. 2005, AJ, 129, 979
Zhu, L. Y., Qian, S. B., Soonthornthum, B., He, J. J., & Liu, L. 2011, AJ, 142, 124